scientific reports

Check for updates

OPEN

Cholesterol metabolism and neuroinflammatory changes in a non-human primate spinal nerve ligation model

Hiroshi Yamane[1,2]✉, Suguru Koyama[1], Takayuki Komatsu[1], Tomoya Tanaka[1], Riyu Koguchi[2], Haruhisa Watanabe[2], Mai Nishiura[2], Satoru Yoshikawa[1]✉ & Tadahiro Iimura[2]✉

Neuropathic pain remains one of the major neurological conditions with high unmet medical needs. Poor translation from preclinical studies using rodent models to clinical trials is one of the major obstacles to the development of new pharmacological medications to treat neuropathic pain. The aims of this study were to establish a behavioral test to evaluate spontaneous pain in a spinal nerve ligation (SNL) model using cynomolgus monkey as a non-human primate (NHP) model. After right unilateral L7 SNL surgery in cynomolgus monkeys, the percentage of weight-bearing on ipsilateral hindlimb significantly decreased, which was well-associated with an analytical score of electroencephalography (EEG). Transcriptomic analysis of RNA-seq results from the dorsal part of the spinal cord identified pathways matching those in equivalent rodent models, along with NHP-specific pathways, suggesting that neuroinflammation and cholesterol transportation/metabolism were the main pathways altered in this NHP model. Additionally, several upregulated genes observed here were previously reported uniquely in clinical studies, but not in rodent models. This study provides a potentially useful model that can aid our understanding of pathophysiological mechanism of neuropathic pain and the development of pain relief therapies by inducing a robust behavioral phenotype and changes in gene expression resembling those in patients.

Keywords Neuropathic pain, Translation, Neuroinflammation, Non-human primate

Abbreviations

SNL	Spinal nerve ligation
NHP	Non-human primate
EGG	Electroencephalography
PSD	Power spectral density
RNA-Seq	RNA sequencing
DEGs	Differentially expressed genes
i.m.	Intramuscular
i.v.	Intravenous
TPM	Transcripts per million
MHC	Major histocompatibility complex
CSF	Cerebrospinal fluid
DRG	Dorsal root ganglion
PNI	Peripheral nerve injury
CRPS	Complex regional pain syndrome
LBP	Low back pain

Neuropathic pain is caused by a lesion or disease of the somatosensory system and affects 7–10% of the general population[1]. Patients with neuropathic pain often experience reduced physical activity, sleeping disorders, depression, and anxiety, which impair their quality of life, thus increasing medical costs[2]. Furthermore,

[1]Pharmaceuticals Research Center, Asahi Kasei Pharma Corporation, 632-1 Mifuku, Izunokuni, Shizuoka 410-2321, Japan. [2]Department of Pharmacology, Faculty and Graduate School of Dental Medicine, Hokkaido University, Sapporo 060-8586, Japan. ✉email: yamane.hf@om.asahi-kasei.co.jp; yoshikawa.sh@om.asahi-kasei.co.jp; iimura@den.hokudai.ac.jp

gabapentinoid analgesic drugs such as pregabalin and mirogabalin that are currently available for those patients show limited efficacy, with pregabalin being effective in only around 3 to 4 out of 10 patients treated[3,4]. Therefore, there is still a substantial unmet need for better pain relief therapies.

Although extensive efforts have been made to develop new pharmacological medications to treat neuropathic pain, a very low success rate in clinical trials has presented an huge obstacle in the field of pain management[4,5]. Specifically, new pain drugs have been associated with significantly low rates of success in phase II and III trials, compared with those for drugs developed to treat other diseases[5], suggesting the extreme difficulty associated with proof-of-concept studies for the treatment of neuropathic pain. Possible factors making these clinical trials difficult include the strong effect of placebos on the symptom of pain, the heterogeneity of patients' pathology, and differences in the assessment of drug efficacy among clinical trials[6–9]. Another issue to be overcome is poor translation from preclinical studies to clinical trials, with many new candidate compounds effective on neuropathic pain model animals showing limited or no effect on patients[6,10–12]. This is potentially attributable to distinct ways of scoring pain in animal models and patients. For example, evoked pain such as hyperalgesia and allodynia induced by mechanical or thermal stimulation is assessed in animal models, while the primary endpoint of clinical trials is spontaneous and continuous pain[10]. Another factor potentially contributing to the discrepancy in efficacy of pain medications between model animals and patients is inter-species differences in the pathophysiological mechanism in sensing and generating pain. Most preclinical studies on neuropathic pain have been conducted using rodent models, which share some pathophysiological features with humans but are reported to differ in their genetics and nervous system, therefore possibly leading to difficulties in precisely predicting drug efficacy in humans. There thus remains a major need to establish animal models and outcome measures that more closely resemble the human setting, which should in turn improve translation in pain therapeutic research.

Several studies have aimed at establishing models of neuropathic pain using non-human primates (NHPs), which are more similar in terms of nervous system structure/function and genetics to humans than rodents are[13–18]. These studies reported that behavioral, electrophysiological, and functional alterations in the nervous system in NHP pain models strongly resemble those in human patients. However, it has yet to be fully elucidated whether neuropathic pain models using NHPs robustly reflect spontaneous pain-related behavior in patients, and more precisely model the pathophysiological features of neuropathic pain especially at molecular level than rodent models.

This study aimed to establish a behavioral test to evaluate spontaneous pain in a spinal nerve ligation (SNL) model by using cynomolgus monkeys as an experimental model NHP with a close genetic background to that of humans. We further conducted RNA-seq analysis on the dorsal horn of the spinal cord to reveal changes in transcriptomic profile to evaluate the molecular aspects of the pathophysiology of neuropathic pain in this model. Furthermore, bioinformatics was used to compare the molecular signatures with those in previously reported corresponding rodent models and human patients.

Results

Changes in weight-bearing after SNL surgery in cynomolgus monkeys

We conducted weight-bearing tests in cynomolgus monkey before and 1, 2, and 3 months after SNL surgery to assess spontaneous pain-related behavior (Fig. 1a). The percentage of weight-bearing on the ipsilateral (right) hindlimb decreased after SNL surgery compared with that preoperatively, and the difference was statistically significant until 2 months after the surgery (Fig. 1b). At 3 months after the surgery, the significant difference was not observed possibly because some animals showed a tendency to recover.

The effect of pregabalin treatment in the SNL monkey model

We next evaluated the effect of pregabalin treatment using 3 animals with retained pain-like behavior at 3 months after the surgery. The percentage of weight-bearing on the ipsilateral hindlimb was assessed before and after the vehicle or pregabalin treatment (Fig. 1c). As a result, the percentage of weight-bearing on the ipsilateral (right) hindlimb in the pregabalin treated group tented to be recovered compared to that in the vehicle control group, albeit not significantly.

The correlation between mean theta power in EEG and behavioral change after SNL surgery in cynomolgus monkeys

To further confirm if the phenotype in cynomolgus monkeys induced by SNL surgery reflects the pathophysiologic nature of neuropathic pain, we conducted electroencephalography (EEG) recording at 1, 2, and 3 months after SNL surgery. The power spectral density (PSD) analysis was performed using the data from C3 electrode (Fig. 2a) corresponding to primary somatosensory area. Then we evaluated the correlation between mean theta power in EEG and the percentage of weight-bearing on the ipsilateral (right) hindlimb. The mean theta power and percentage of weight-bearing on the ipsilateral (right) hindlimb were pooled from 1 to 3 month after the SNL surgery, and Spearman's rank correlation coefficient was calculated. The mean theta power negatively correlated with the weight bearing on ipsilateral hindlimb significantly, suggesting the animals with stronger pain-like behavior have stronger mean theta power (Fig. 2b).

To investigate if the SNL surgery affects sleeping/waking cycles of the animals, we measured the sleeping/waking time and cycles at 1, 2, and 3 months after the surgery. Those data were pooled from 1 to 3 month after the SNL surgery, and Spearman's rank correlation coefficient between the percentage of weight-bearing on the ipsilateral hindlimb and the Sleeping/waking time or cycles were calculated. The sleeping and waking time negatively and positively correlated with the weight bearing on ipsilateral hindlimb, respectively (Fig. 2c). On the other hand, the number of sleeping/waking cycles did not significantly correlate with the weight bearing (Fig. 2c).

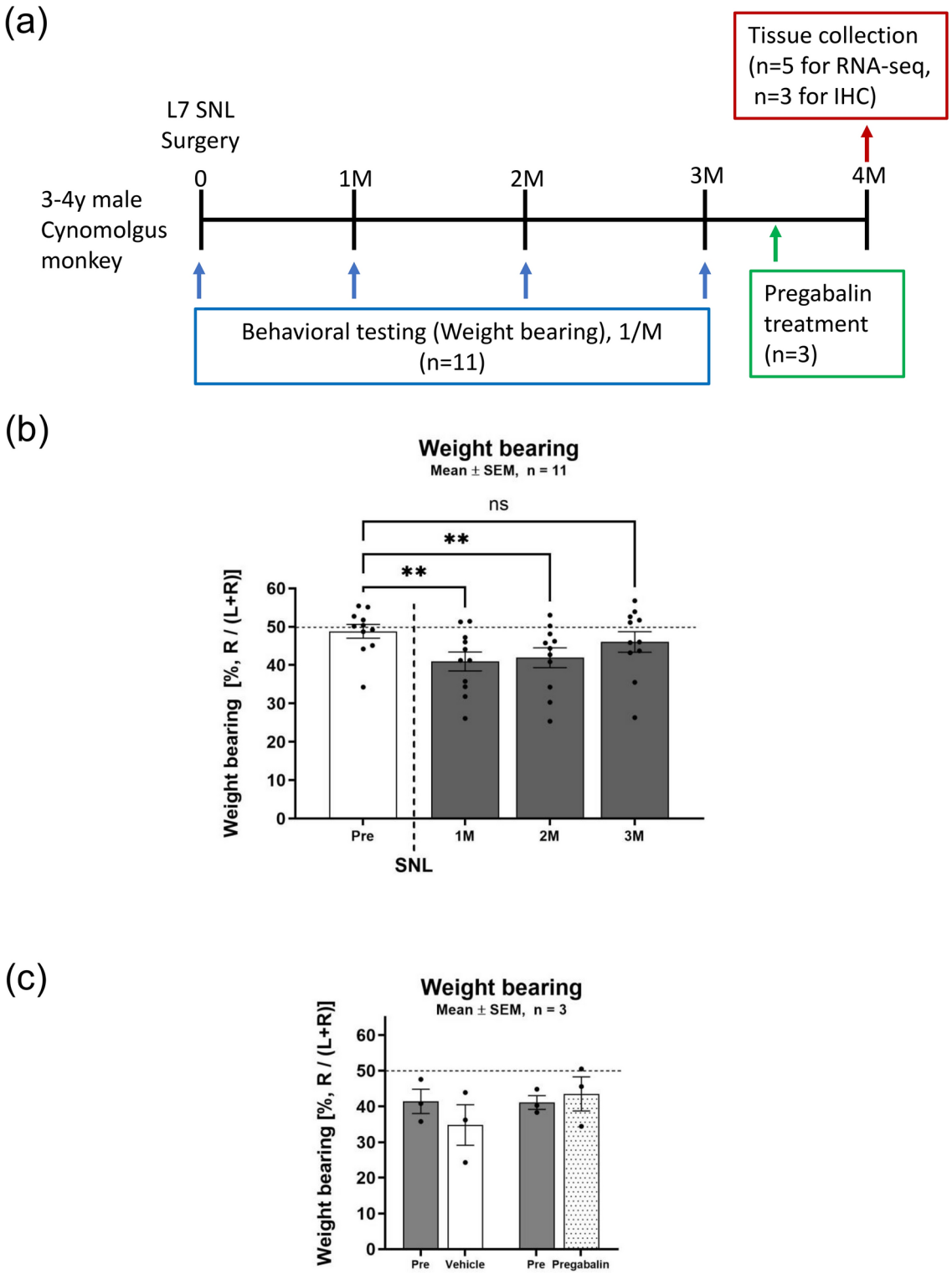

Fig. 1. Experimental schedule and weight-bearing tests. (**a**) The schedule of the experiments and sampling. The schedule of SNL surgery, behavioral testing, and sampling is shown. (**b**) Spinal nerve ligation in cynomolgus monkeys induces a decrease in weight-bearing of ipsilateral hindlimb. The weight-bearing tests were conducted before (pre) and 1, 2, and 3 months after SNL surgery. The percentage of weight-bearing on ipsilateral (right) hindlimb was calculated using the following formula: Weight-bearing [%, R / (L + R)] = ipsilateral weight-bearing (kg) × 100 / [ipsilateral weight-bearing (kg) + contralateral weight-bearing (kg)]. It significantly decreased 1 and 2 months after SNL surgery compared with that before surgery. **: $p < 0.01$, ns: not significant. Data are presented as mean ± SD. R: right, L: left.

(a)

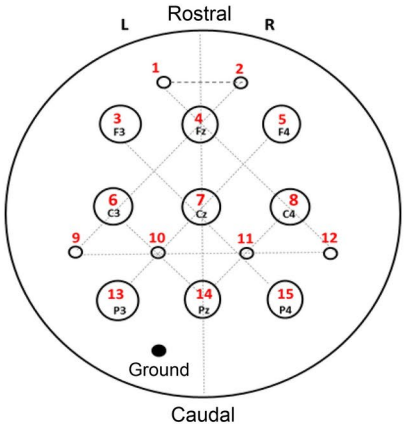

(b)

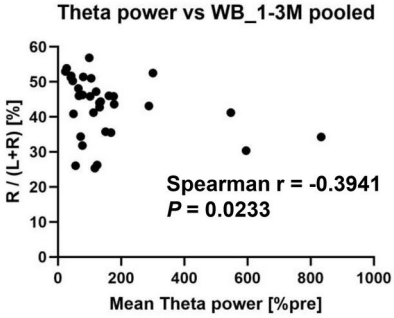

(c)

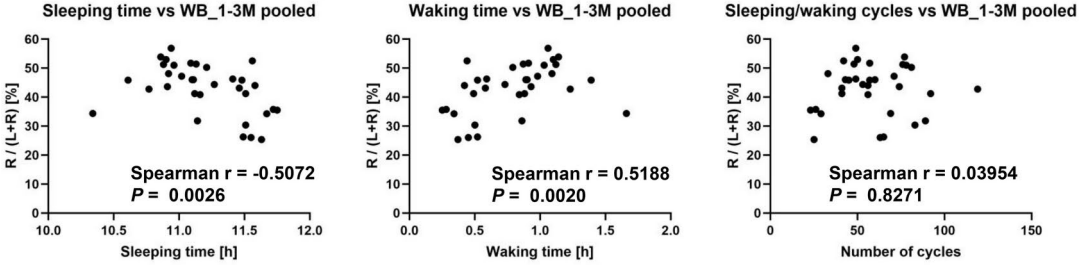

(d)

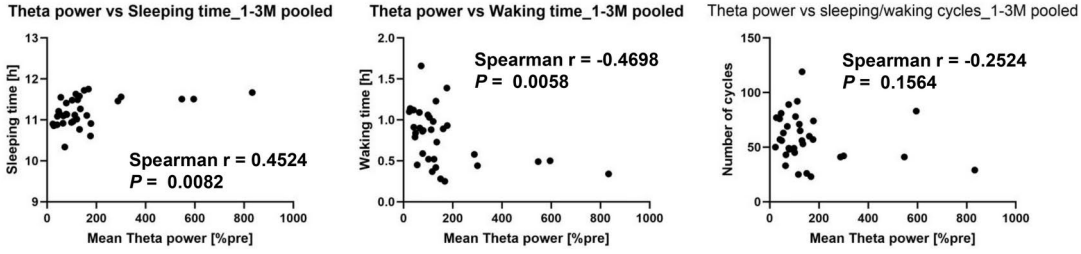

To see if the mean theta power and sleeping/waking cycles are related to each other after the SNL surgery, the correlation of those was evaluated. The sleeping and waking time positively and negatively correlated to the mean theta power, respectively (Fig. 2d). On the other hand, the number of sleeping/waking cycles did not significantly correlate with the mean theta power (Fig. 2d).

Changes in dorsal spinal cord gene expression profiles in SNL monkey model

To investigate the molecular aspects of the pathophysiology in the SNL monkey model, we conducted transcriptomic analysis of RNA-seq results in the dorsal part of the spinal cord, and compared gene expression levels on the ipsilateral (right) and contralateral (left) sides to calculate the fold change of expression of each gene. We set thresholds of adjusted $p < 0.01$ and absolute log2(fold change) ≥ 0.5 to define differentially expressed

◀**Fig. 2**. The correlation between mean theta power in EEG and behavioral change after SNL surgery. (**a**) The schematic drawing of the electrodes location in the monkey skull for EEG recording. Under anesthesia, 16 stainless steel screw electrodes were placed over the skull corresponding to international 10-20 system. (**b**) The mean theta power in EEG negatively correlated to the weight bearing on ipsilateral hindlimb significantly. The EEG recording was conducted at 1, 2, 3 month after surgery and then the data were pooled, and the correlation with behavioral changes (weight bearing and sleeping/waking cycles) were evaluated by using Spearman's rank correlation. (**c**) The correlation between sleeping/waking cycles and weight bearing. The sleeping/waking time and cycles during a dark period (12h, 19:00-7:00) was measured at 1, 2, 3 month after surgery and then the data were pooled, and the correlation with weight bearing was evaluated. The sleeping and waking time negatively and positively correlated with the weight bearing on ipsilateral hindlimb, respectively. (**d**) The correlation between mean theta power and sleeping/waking cycles. The sleeping and waking time positively and negatively correlated with the mean theta power, respectively.

genes (DEGs, Fig. 3a and Table 1) in this study, with 40 DEGs being identified from among the 12,714 genes analyzed.

DEGs with $p < 0.01$ and absolute log2(fold change) ≥ 0.5 were functionally annotated and clustered by the GO Biological Processes, Reactome Gene Sets, KEGG Pathways, and CORUM with Metascape webtool. The top 20 enriched terms or pathways are shown in Fig. 3b as a heatmap colored by p-value, and a subset of representative terms from the full cluster converted into a network layout is shown in Fig. 3c. The Metascape analysis revealed that the DEGs between the ipsilateral and contralateral samples were significantly associated with antigen processing and presentation of exogenous peptide antigen via major histocompatibility complex (MHC) class II (GO:0019886), regulation of cell activation (GO:0050865), NABA Matrisome (M5885), Classical antibody-mediated complement activation (R-HSA-173623), NR1H3 & NR1H2 regulation of gene expression linked to cholesterol transport and efflux (R-HSA-9029569), and interleukin-10 signaling (R-HSA-6783783) [−log10(p-values) > 6].

The DEGs upregulated in the ipsilateral spinal cord included those related to immunity and the inflammatory system such as *Slamf7*, *Timp1*, *Ccl19*, *Ccl2, Mdk*, and *Tnfrsf1b* are known to encode cytokines, chemokines, or a cytokine receptor (Fig. 4a). Genes related to the complement system, such as *C1qa*, *C1qc*, and *Serpinf1*, were also upregulated in the ipsilateral spinal cord of the monkey SNL model in this study (Fig. 4b). Genes of *Cd74*, *Hla-dma*, and *Ifi30* are related to antigen recognition by MHC class II, all of which were found to be upregulated in the ipsilateral spinal cord (Fig. 5a). Another group of genes upregulated in the ipsilateral spinal cord included *Abca1, Apoc1, Apod*, *Nr1h3, Msmo1*, *Apoe, Idi1,* and *Apol2* which were involved in cholesterol transportation and metabolism (Fig. 5b).

Next, to evaluate whether the SNL model using cynomolgus monkey has a molecular basis resembling the pathophysiology of patients with neuropathic pain, DEGs for which there is known evidence of a change in expression level in the tissue or concentration in body fluid of such patients were compiled, as shown in Table 2.

All genes listed in Table 2 are upregulated in the ipsilateral dorsal part of the spinal cord compared with the level in the contralateral one in the monkey SNL model in this study. These genes are also reported to be upregulated or correlated with the symptom of pain in patients with pain-related disorders, except for serpinF1, the level of which is decreased in the cerebrospinal fluid (CSF) of patients with neuropathic pain.

Immunofluorescence analyses of GFAP and LXRα

To validate our SNL monkey model and RNAseq analysis, we conducted immunofluorescence analyses using anti-GFAP and anti-LXRα (encoded by *Nr1h3*) antibodies (Fig. 6). Specificities of these antibodies were confirmed by comparing the results with those using nonspecific IgG as negative controls (Supplementary Fig. 1). AI-driven automatic segmentations were conducted to binarize antibody-derived signals, and fluorescence intensity in on the ipsilateral (right) and contralateral (left) dorsal horn were compared (Supplementary Fig. 2). GFAP-derived signal was significantly upregulated in in the ipsilateral side compared to that in the contralateral (left) side, confirming a neuroinflammatory phenotype in the ipsilateral side induced by the SNL (Fig. 6a). LXRα-derived signals were tended to be augmented in the ipsilateral side, albeit not significantly, supporting the findings by our RNAseq analysis.

Discussion

In this study, we observed pain-related behavioral changes in a SNL monkey model using a weight-bearing test. After the SNL surgery, the animals showed decreased weight-bearing in the ipsilateral hindlimb, in which the primary afferent fibers from the ganglion just proximal to the ligated L7 spinal nerve were distributed. This trend was statistically significant from 1 to 2 months postoperatively, suggesting the long-term persistence of neuropathic pain. At 3 months after the surgery, some animals showed a tendency to recover. This could have been due to individual variability in pain intensity or pathophysiology induced by SNL surgery, or insensitivity induced by neuronal/axonal degeneration in the peripheral nerve after long-term stress by chronic ligation of the spinal nerve. Pregabalin treatment at 3 months after the SNL surgery did not show a significant effect on pain-like behavior of the model. This could be due to a small number of animals used because this timepoint shows tendency of recovery from pain-like behavior, or it might be reflecting the existence of pregabalin non-responder as reported in clinical situation. However, further study using more animals and timepoints is needed to conclude the validity of this model for pharmacological evaluation. Furthermore, due to a limited number of animals, we assessed the effect of SNL surgery on pain-like behavior by intra-individual comparison to minimize

(a)

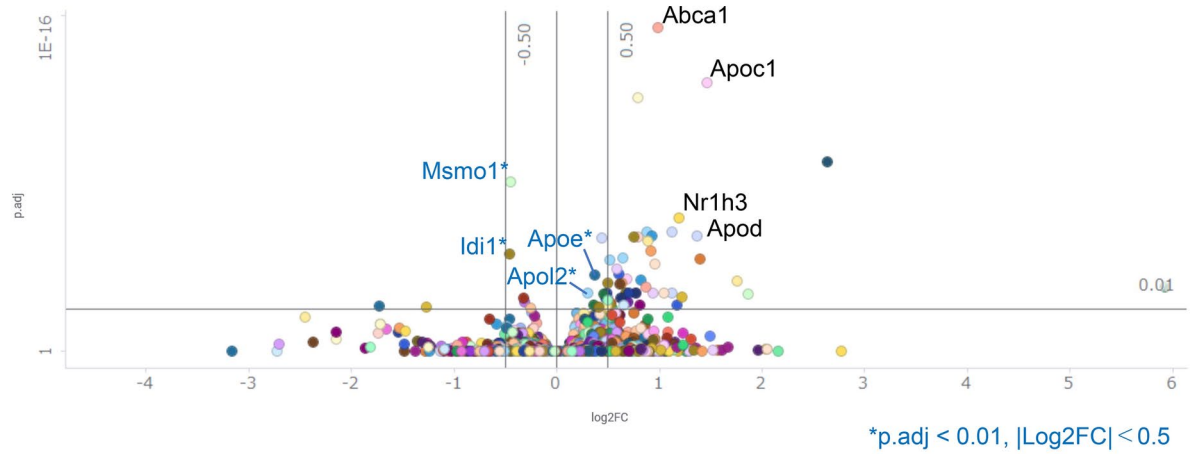

(b)

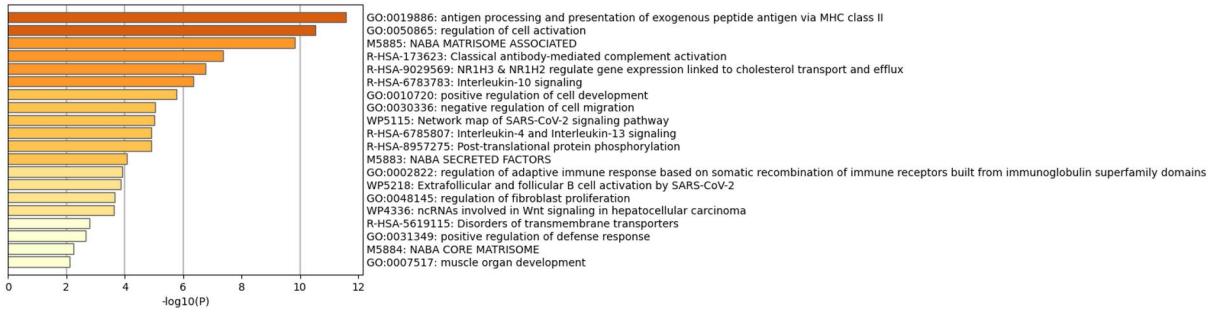

(c)

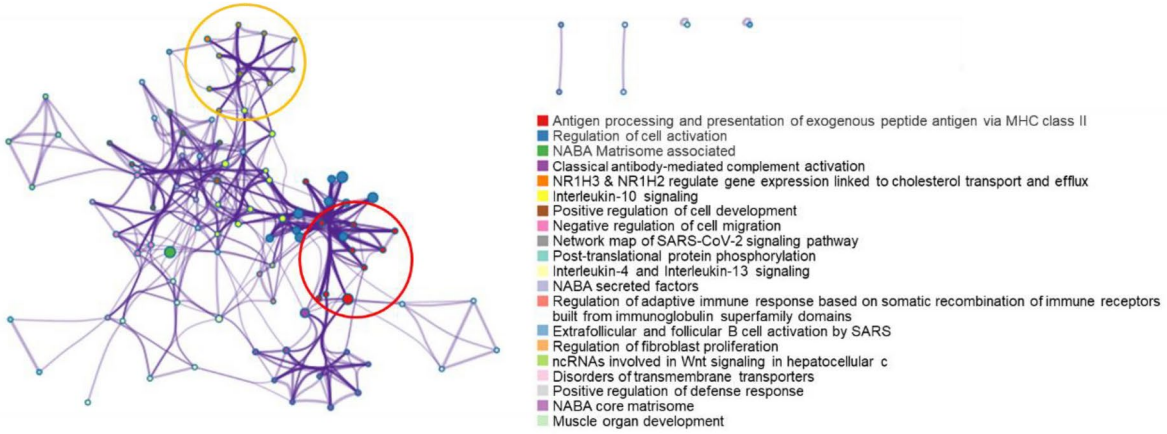

the effect of inter-individual variation. Thus, additional controls such as sham operation will be required in the future study to improve the reliability of our findings above.

To further investigate if the SNL surgery induce pain-related change in the function of central nervous system of cynomolgus monkeys, we conducted EEG recording/PSD analysis and sleeping/waking time measurement. After the SNL surgery, the animals showed a significant negative correlation between the mean theta power in EEG analysis and the percentage of weight bearing on ipsilateral (right) hindlimb. It suggests the animals with stronger pain-like behavior (lower percentage of weight bearing on ipsilateral hindlimb) had stronger mean theta power in EEG. This is in accordance with the previous studies which reported the increased theta power in EEG or magnetoencephalography (MEG) analysis in patients with chronic pain including neuropathic pain[19–22] and animal models of chronic pain[23–25]. Thus, the monkey SNL model in this study is also suggested to share the similar electrophysiological phenotype with that in patients with neuropathic pain and previous animal models.

◀**Fig. 3**. Transcriptional profile changed in the ipsilateral dorsal part of the spinal cord compared with that in the contralateral part by RNA-seq analysis. (**a**) Volcano plot for all genes identified in the SNL monkey model. Each plot represents a single gene. The names of representative genes related to cholesterol metabolism, transportation, or homeostasis are shown. Gene names with asterisks are genes with $p < 0.01$ and absolute log2(fold change) < 0.5, and those without asterisks are DEGs with $p < 0.01$ and absolute log2(fold change) ≥ 0.5. The p-values are adjusted for multiple comparisons. (**b**) A heatmap of enriched terms across input gene lists, colored by p-values. DEGs with $p < 0.01$ and absolute log2(fold change) ≥ 0.5 were functionally annotated and clustered by the GO Biological Processes, Reactome Gene Sets, KEGG Pathways[71–73], and CORUM with Metascape webtool (v3.5.20230623, http://metascape.org/). (**c**) A network of representative enriched terms. A subset of representative terms from the full cluster converted into a network layout by using Metascape webtool (v3.5.20230623, http://metascape.org/) is shown. Each term is represented by a circle node, where its size is proportional to the number of input genes falling under that term, and its color represents its cluster identity (i.e., nodes of the same color belong to the same cluster). Terms with a similarity score > 0.3 are linked by an edge (the thickness of the edge represents the similarity score). The network is visualized with Cytoscape with "force-directed" layout and with edges bundled for clarity. One term from each cluster is selected to have its term description shown as a label. Red circle indicates a representative cluster related to antigen processing and presentation of exogenous peptide antigen via MHC class II (GO:0,019,886), and yellow circle indicates a cluster related to NR1H3 & NR1H2 regulation of gene expression linked to cholesterol transport and efflux (R-HSA-9029569).

Because a sleep disturbance is associated with neuropathic pain[26], we hypothesized the monkey SNL model in this study might also show sleeplessness. However, to our surprise, the sleeping time and waking time during dark period showed negative and positive correlation with the percentage of ipsilateral weight bearing, respectively, suggesting the animals with stronger pain-like behavior have longer sleeping time. The similar correlation was also observed between sleeping/waking time and the mean theta power. Although the exact mechanism of this apparent discrepancy is not clear, because we evaluated sleeping/waking time just by the visual inspection (i.e. animals' motion), it cannot be denied that the decrease of spontaneous locomotor activity or psychological changes induced by SNL affected the result. The decrease of locomotive activity was reported in neuropathic pain model[27]. In addition, hypersomnia was reported to be comorbid with mood disorders[28], which also often comorbid with chronic pain. The sleep disturbance in patients and animal models of chronic pain can be assessed by NREM and REM duration[26]. While we conducted EEG/PSD analysis only in awake and resting states because of technical limitation of our EGG recording system, the future development of measurement system to evaluate EEG in sleeping state combined with this model animals should be a solution to discover the exact effect of SNL on sleep. Such system will enable us to distinguish between the sleeping state and locomotive activity, and more directly evaluate the effect on REM/NREM sleep states.

To further evaluate our monkey SNL model regarding the molecular basis of the pathophysiology, we investigated changes in gene transcriptional profile in the ipsilateral dorsal part of the spinal cord compared with that in the contralateral part by RNA-seq analysis. A total of 40 genes exhibited significant changes in their expression level with adjusted $p < 0.01$ and absolute log 2 (fold change) ≥ 0.5. Those genes showed strong associations with the activation of innate and acquired immunity such as antigen processing and presentation, complement system activation, and IL-10 signaling, and with cholesterol transport (Figs. 3, Tables 1 and 2).

The DEGs upregulated in the ipsilateral spinal cord included those related to immunity and the inflammatory system. Among them, *Slamf7*, *Timp1*, *Ccl19*, *Ccl2, Mdk*, and *Tnfrsf1b* are known to encode cytokines, chemokines, or a cytokine receptor. These genes were all upregulated in the ipsilateral dorsal spinal cord in the monkey SNL model (Fig. 4a). *Slamf7* encoding SLAM Family Member 7, was reported to be upregulated in the dorsal root ganglion (DRG) of a mouse model of complex regional pain syndrome (CRPS)[29]. In addition, SLAMF7 protein was reportedly expressed in plasma cells in synovial tissues of patients with rheumatoid arthritis[30]. *Timp1* mRNA expression was reportedly increased in the spinal cord of a mouse model of spinal cord injury[31]. The plasma concentration of TIMP1 protein in patients with chronic neuropathic lower-back pain was also reported to be increased compared with that in healthy controls and patients with chronic inflammatory lower-back pain[32]. Moreover, a change in the serum concentration of CCL19 protein was reported to be associated with a change in the progression of lower-back pain, with a decrease in its level being associated with less pain after 1 year follow-up[33]. Furthermore, cerebrospinal fluid and plasma concentrations of CCL19 were increased in patients with neuropathic pain[34,35]. CCL2 protein expression in the DRG of a rat model of neuropathic pain was also increased compared with that in sham or intact animals[36]. Meanwhile, CCL2 was reported to induce the activation of microglia and pain-like behavior in naïve rats after intraspinal injection. Finally, minocycline and CCR2 (receptor of CCL2) antagonist were reported to attenuate pain-like behavior when intrathecally injected into a rat model of neuropathic pain[37]. These reports suggest that CCL2 may be involved in the pathophysiology of neuropathic pain via microglial activation. *Mdk* encodes midkine, a secreted protein that functions as a cytokine and growth factor. It was reported that midkine was detected in the synovial fluid of patients with rheumatoid arthritis and osteoarthritis, whereas it was not detected in healthy controls[38]. In contrast, conflicting findings have been reported on the changes in expression levels of *Mdk* and midkine protein in neuropathic pain animal models[39,40]. To the best of our knowledge, no reports suggesting that midkine level is altered in human patients with neuropathic pain have yet been published. Thus, the involvement of midkine in the pathophysiology of neuropathic pain remains to be investigated in clinical settings. *Tnfrsf1b* encodes tumor necrosis factor receptor 2 (TNFR2), also known as p75 or CD120b. *Tnfrsf1b* mRNA was reported to be upregulated in the whole blood of patients with chronic pain[41] and in the spinal cord of a rat model of neuropathic pain[42]. TNFR2 is also known to

Gene symbol	Log2(fold change)	*p*.val	p.adj
ABCA1	0.981566	2.36E-20	3.84E-16
APOC1	1.467191	1.97E-17	1.60E-13
HLA-DRA	0.789252	1.60E-16	8.68E-13
SLAMF7	2.636462	2.27E-13	9.25E-10
NR1H3	1.187395	1.58E-10	4.28E-07
C1QA	0.87928	9.31E-10	1.99E-06
NGFR	1.120804	9.79E-10	1.99E-06
TIMP1	0.924869	1.74E-09	3.14E-06
APOD	1.369572	2.04E-09	3.33E-06
SFRP4	0.784688	2.50E-09	3.70E-06
FOXD3	0.891533	4.89E-09	5.69E-06
C1QC	0.916366	1.49E-08	1.62E-05
HLA-DMA	0.646108	3.85E-08	3.69E-05
GPNMB	1.398485	4.42E-08	4.00E-05
TNFRSF1B	0.514745	5.56E-08	4.77E-05
C1S	0.953528	8.63E-08	7.03E-05
IFI30	0.584047	1.66E-07	0.000129
FCER1G	0.606906	2.99E-07	0.000221
CD74	0.680602	5.22E-07	0.000354
PCOLCE	0.816872	6.28E-07	0.00041
CCL19	1.75442	7.03E-07	0.000441
IGFBP4	0.634759	9.75E-07	0.000568
FZD2	0.614301	1.12E-06	0.000629
SERPINF1	0.865997	1.68E-06	0.0009
CLEC6A	5.922619	1.71E-06	0.0009
F13A1	1.123462	3.58E-06	0.001632
OLFML2B	0.773247	3.52E-06	0.001632
ITIH2	0.77348	3.52E-06	0.001632
COL6A3	1.043134	4.03E-06	0.001728
S100A4	0.69794	4.31E-06	0.001756
FCRL5	1.866947	4.66E-06	0.001853
CCL2	1.219383	7.32E-06	0.002775
HLA-DMB	0.626508	8.99E-06	0.003118
CD48	0.689821	1.36E-05	0.004458
CP	1.168701	2.01E-05	0.006289
EFNB1	0.528398	2.21E-05	0.006563
STING1	0.655298	2.15E-05	0.006563
MDK	0.811414	2.26E-05	0.006583
SLC5A7	-1.7329	2.49E-05	0.006985
CHODL	-1.26961	2.76E-05	0.007626

Table 1. The DEGs with $p < 0.01$ and absolute log2(fold change) ≥ 0.5.

mediate NGF and BDNF signaling as their low-affinity receptor, which plays a crucial role in the pathophysiology of neuropathic pain[43]. Cytokines and chemokines are known to be secreted from neurons after nerve injury. At the spinal cord level, cytokines and chemokines including TNFα and CCL2 activate microglia and astrocytes, which may enhance neuroinflammation[44] and maintain hyperactivated nociception in neuropathic pain. It is thus suggested that the monkey SNL model in this study shares a pathogenic mechanism with neuropathic pain that involves cytokines and chemokines and their proinflammatory effects.

Genes related to the complement system, such as *C1qa*, *C1qc*, and *Serpinf1*, were also upregulated in the ipsilateral spinal cord of the monkey SNL model in this study (Fig. 4b). *C1qa* and *C1qc* encode complement C1q A chain (C1QA) and C1q C chain (C1QC), respectively. C1Q was reported to be upregulated in the ipsilateral dorsal horn of a mouse model of neuropathic pain[45]. The expression of *C1qa* mRNA was also shown to be upregulated in the DRG of patients with neuropathic pain[46]. Meanwhile, the expression of C1QC protein and *C1qc* mRNA was found to be upregulated in the plasma of patients with fibromyalgia[47] and in the spinal cord of a rat model of neuropathic pain[42,48], respectively. *Serpinf1* encodes pigment epithelium-derived factor (PEDF), which exerts antiangiogenic and neurotrophic effects, while also activating the classical complement pathway. It was also reported that the expression of PEDF protein was upregulated in the peripheral nervous system

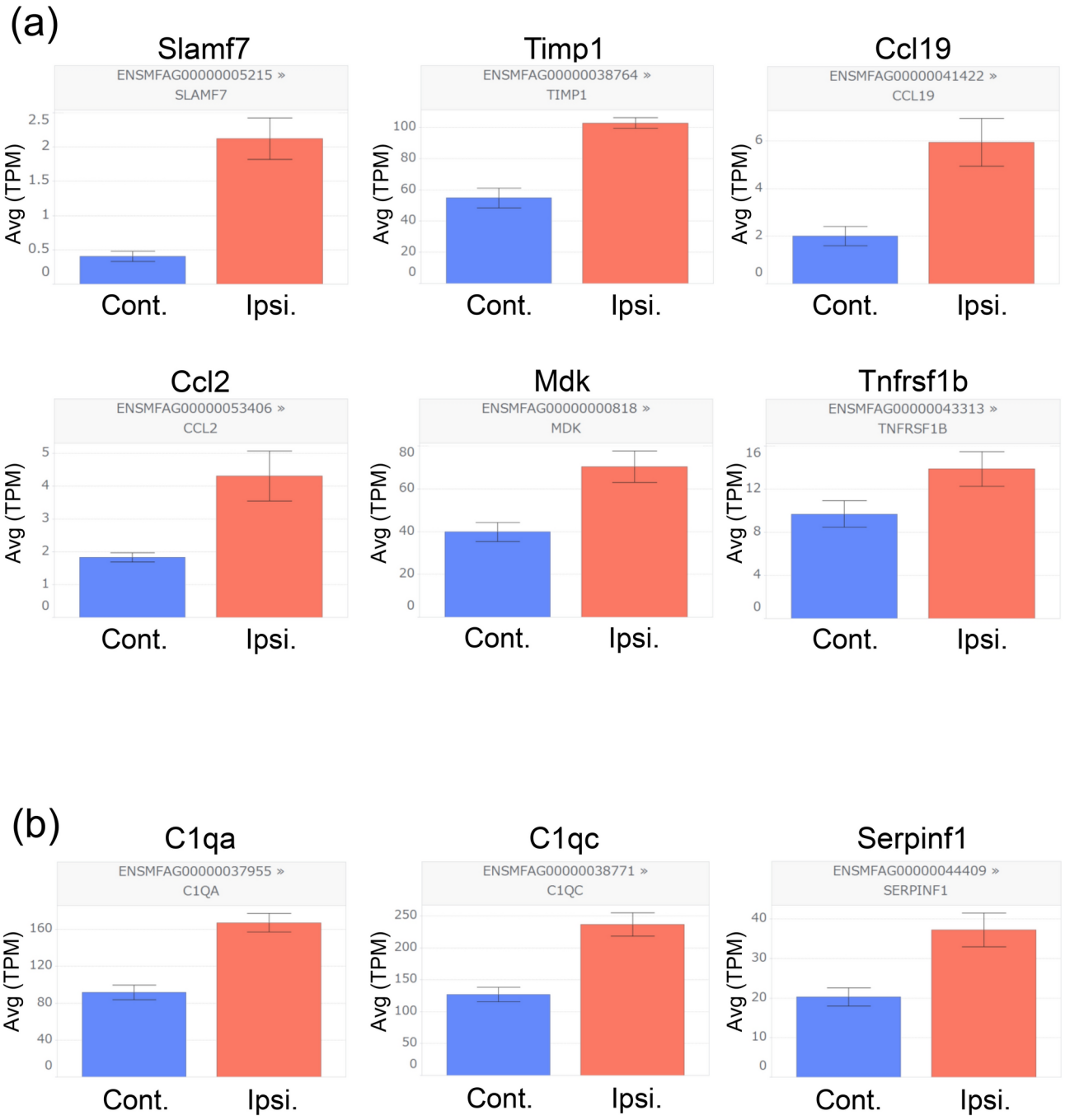

Fig. 4. Relative expression levels of genes related to the inflammatory and complement systems. (**a**) Genes related to immunity and the inflammatory system such as *Slamf7*, *Timp1*, *Ccl19*, *Ccl2*, *Mdk*, and *Tnfrsf1b* were upregulated in the ipsilateral spinal cord. (**b**) Genes related to the complement system such as *C1qa*, *C1qc*, and *Serpinf1* were upregulated in the ipsilateral spinal cord.

of a mouse model of neuropathic pain[49]. Meanwhile, the expression of PEDF protein was downregulated in the cerebrospinal fluid of patients with neuropathic pain[50], but was upregulated in the cartilage of patients with osteoarthritis[51]. Thus, the involvement of PEDF in the pathophysiology of neuropathic pain should be elucidated. The complement system plays roles in the immune system and the activation of microglia. The C1Q pathway is known to contribute to synaptic remodeling and regulation of axonal growth and neuronal survival[52]. Thus, the increase of C1Q expression after nerve injury may be an adaptive mechanism to enhance nerve regeneration. Meanwhile, C1Q was reported to induce the activation of microglia and their proinflammatory response[53], which plays a crucial role in the pathology of neuropathic pain. Thus, although the exact role is yet to be investigated, activation of the complement pathway may have both protective and destructive roles in the pathophysiology of the monkey SNL model in this study.

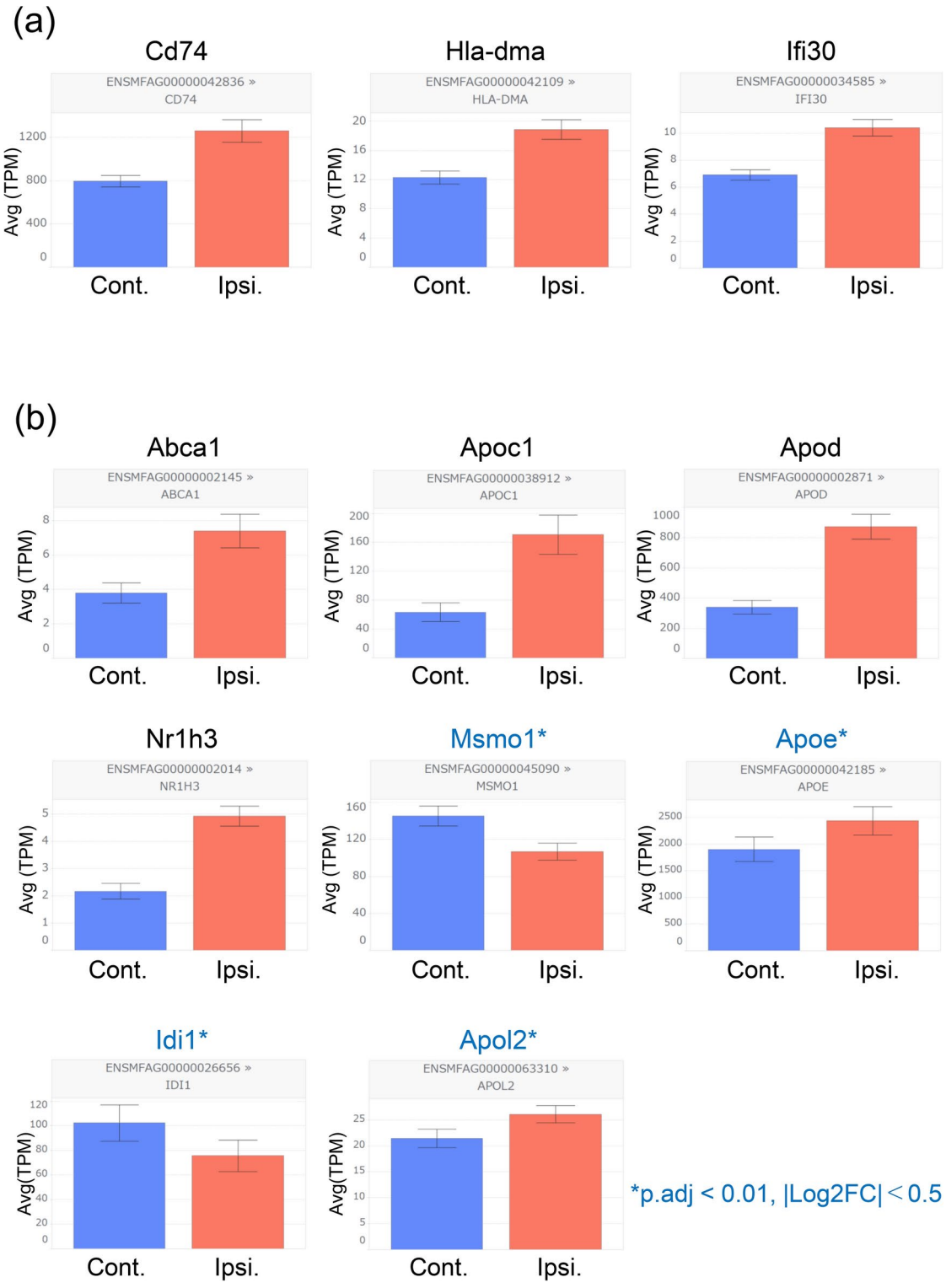

Fig. 5. Relative expression levels of genes related to antigen recognition and cholesterol transportation. (**a**) Genes related to antigen recognition by MHC class II such as *Cd74*, *Hla-dma*, and *Ifi30* were upregulated in the ipsilateral spinal cord. (**b**) Genes related to cholesterol transportation such as *Abca1*, *Apoc1*, *Apod*, and *Nr1h3* were upregulated in the ipsilateral spinal cord.

Cd74, *Hla-dma*, and *Ifi30* are related to antigen recognition by MHC class II. All of these genes were found to be upregulated in the ipsilateral spinal cord in the monkey SNL model in this study (Fig. 5a). *Cd74* encodes a protein associated with MHC class II. The expression of *Cd74* mRNA was reported to be upregulated in the DRG and spinal cord of rat models of neuropathic pain[54,55] and in the DRG of patients with neuropathic pain[46].

Gene symbol	Evidence in rodent pain models	Clinical evidence		
		Disease	Sample	Changes reported
Apoc1	–	Neuropathic pain and fibromyalgia	CSF	Upregulated[20]
Slamf7 (CD319)	Upregulated in DRG of CRPS mice[21]	Rheumatoid arthritis	Synovial tissue	Expressed in synovial tissue[22]
C1qa	Increased C1Q(+) synapses in dorsal horn of PNI rats[23]	Neuropathic and chronic pain	DRG	Increased[24]*
Timp1	Upregulated in spinal cord of CCI[25]** and SCI rats[26]	Neuropathic lower-back pain	Plasma	Increased[27]
Apod	Upregulated in sciatic nerve of SNI rats[28] and DRG of CCI rats[29]	Lower-back pain	CSF	Increased in patients with painful disc degeneration[30]
C1qc	Upregulated in spinal cord of CCI rats[25,31]	Fibromyalgia	Plasma	Increased[32]
Hla-dma	–	Chronic lower-back pain	Whole blood	Increased compared with in acute LBP[33]
Tnfrsf1b	Upregulated in spinal cord of CCI rats[25]**	CRPS Irreversible pulpitis, lumbar disc prolapse	Whole blood pulp Whole blood	Upregulated[34]
Cd74	Upregulated in DRG of SNI rats[35] and spinal cord of CCI mice[36] and rats[25]**	Neuropathic and chronic pain	DRG	Upregulated[24]*
Ccl19	–	Neuropathic pain Lower-back pain	CSF and serum Serum	Increased[37,38] Low CCL19 correlates with recovery from pain[39]
SerpinF1	Upregulated in spinal cord of CCI rats[25]** and sciatic nerve of SNI rats[40]	Neuropathic pain Osteoarthritis	CSF Cartilage	Decreased[41] Upregulated[42]
Olfml2B	Upregulated in spinal cord of CCI rats[25]**	Osteoarthritis and rheumatoid arthritis	Synovial tissue	Upregulated[43]
Itih2	–	Trigeminal neuralgia	CSF	Increased[44]
Col6a3	–	Osteoarthritis	Cartilage and synovial tissue	Upregulated[45]
Ccl2	Upregulated in spinal cord[25]** and DRG[46] of CCI rats	Osteoarthritis	Synovial fluid	CCL2 level correlates with the symptom of pain[47]
Cp (Ceruloplasmin)	Upregulated in spinal cord of CCI rats[25]**	Chronic widespread pain Fibromyalgia	Plasma Plasma	Correlates with the symptom of pain[48] Increased[49]
Mdk (Midkine)	Unchanged in spinal cord of CCI rats[25,50] Transient increase in spinal cord of SCI rats[51]	Osteoarthritis and rheumatoid arthritis	Synovial fluid	Increased[52]

Table 2. DEGs with evidence of changes in expression in patients with neuropathic pain. -: No reported evidence in rodent pain models. *: From RNAseq data available in dbGaP under accession number phs001158.v2.p1. **: From RNA-Seq data available through the NCBI's Gene Expression Omnibus (GEO) repository (GSE143895).

Meanwhile, *Hla-dma* encodes an HLA class II alpha chain paralog. *Hla-dma* mRNA expression was reported to be upregulated in the whole blood of patients with chronic lower-back pain (LBP) compared with the level in acute LBP[56]. However, whether the expression of Hla-dma changes in a neuropathic pain model has not been reported. Finally, *Ifi30* encodes gamma-interferon-inducible lysosomal thiol reductase (GILT), which is expressed in antigen-presenting cells and is related to antigen processing. It was reported that the expression of *Ifi30* mRNA was upregulated in the spinal cord of a rat model of neuropathic pain[57]. In addition, in a previous report it was suggested that the activation of T helper cells by MHC-II promotes axonal loss and neuropathic pain after neuronal injury[58]. Furthermore, it is known that T cells infiltrate into the central nervous system and interact with microglia through MHC-II, and maintain pain via the secretion of proinflammatory mediators in the setting of neuropathic pain[59]. Taken together, the findings in this study suggest that MHC-II-mediated T-cell activation causing neuroinflammation and neuronal damage may be involved in the pathogenesis in the monkey SNL model in this study. Activation of immunity and the inflammatory system is commonly reported in neuropathic pain models and patients[60], suggesting that the monkey SNL model in this study involves molecular mechanisms matching those in equivalent rodent models and in patients with neuropathic pain.

Unexpectedly, another enriched pathway identified by RNA-seq analysis in this study was cholesterol transportation. Among the DEGs upregulated in the ipsilateral spinal cord in the monkey SNL model in this study, *Abca1, Apoc1, Apod*, and *Nr1h3* are involved in this pathway (Fig. 5b). These genes are also reported to be upregulated in neuropathic pain rodent models and patients[42,61–65]. Moreover, four additional genes were found to exhibit significant changes ($p < 0.01$) and are related to cholesterol metabolism, namely, *Msmo1*, *Apoe, Idi1,* and *Apol2* (Fig. 5b), although they were not included in the enrichment analysis (Fig. 3) because of their relatively small changes [absolute log(fold change) < 0.5]. Our transcriptomic analyses underlined molecular changes in cholesterol transport or metabolism in models of neuropathic pain, which appeared to be novel since no study previously reported their involvement in pain models. Conditional knockdown of the cholesterol transporters ABCA1 and ABCG1 in microglia reportedly induced allodynia in naïve mice[61]. Furthermore, administration of the apoA-I binding protein (AIBP) to chemotherapy-induced peripheral neuropathy (CIPN)

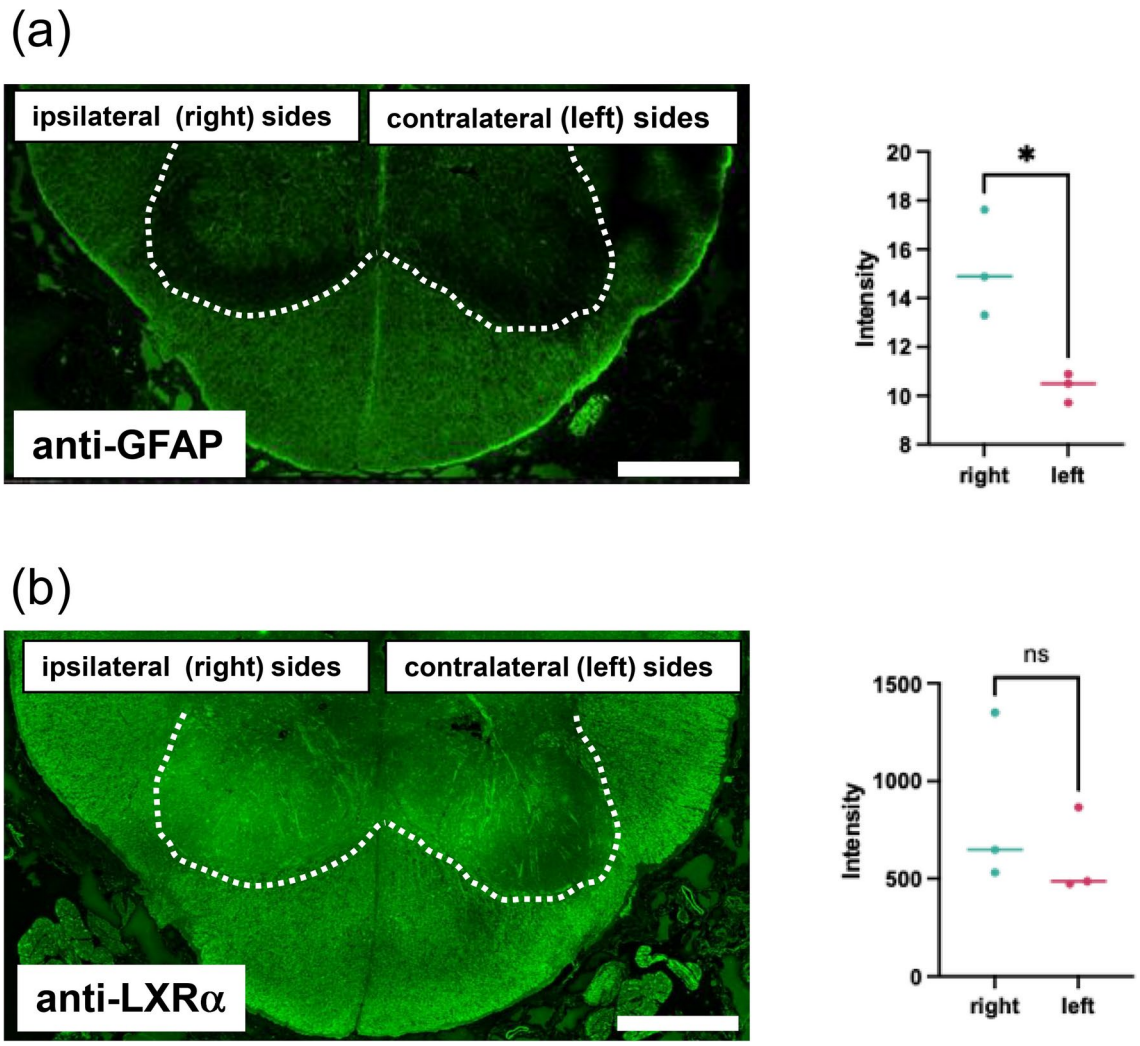

Fig. 6. Comparative analyses of protein expression levels of GFAP and LXRα on the ipsilateral (right) and contralateral (left) dorsal part of the spinal cord. (**a**) GFAP was upregulated in the ipsilateral spinal cord. (**b**) LXRα encoded by *Nr1h3* were upregulated in the ipsilateral spinal cord. White dotted lines demarcate the areas of dorsal horn. Scale bars indicate 500 nm.

model mice facilitated cholesterol depletion from inflammarafts (enlarged, clustered lipid rafts containing elevated cholesterol levels) and attenuated the pain in this model. These findings suggest that cholesterol metabolism plays an important role in neuropathic pain via neuroinflammation and microglia. It is possible that changes in cholesterol homeostasis affect the function of neurons and oligodendrocytes because cholesterol is the major component of the cell membrane and myelin sheaths and plays important roles in neurotransmission and synaptic plasticity[66,67]. Consistent with this, hyperlipidemia has been suggested to be related to the development of diabetic neuropathy[68] and neurodegenerative diseases[69]. It remains to be elucidated whether and how changes in the expression levels of genes related to cholesterol transport and metabolism as seen in this study affect the pathophysiology of neuropathic pain.

Notably, several upregulated genes observed in this study were previously reported uniquely in clinical studies, but not in rodent models. These include *Apoc1, Hla-dma, Itih2, Col6a3*, and *Mdk*. Although the exact functions of these genes in the pathophysiology of pain in humans and NHPs remain to be elucidated, these molecules are likely to mediate the development of neuropathic pain specifically in primates. This indicates that the NHP pain model in this study can at least partly mimic the pathophysiology of patients affected by neuropathic pain and can be useful for elucidation of the difference in pathophysiological mechanism between rodents and primates.

This study has a limitation by using a limited number of animals, a single timepoint, and intra-individual comparison. It is necessary to further evaluate this model by using more animals, timepoints, and additional controls such as sham operation in the future study. It can be helpful for improvement of our understanding of the molecular pathophysiology in this model, as discussed in behavioral analysis. Another limitation is the timepoint of RNA-seq analysis because we showed tendency of recovery in behavioral analysis at 3 months after the surgery, the similar analysis at an earlier timepoint such as at 1 or 2 months after surgery might have been

more informative to evaluate the molecular aspect of pathophysiology in this model. However, we did not recruit another set of experimental monkeys to conduct our RNAseq analysis at an early point from an ethical point of view. Nevertheless, even at 4 months after the surgery, the RNA-seq analysis revealed the similar changes in gene expression profile as reported in patients and models of chronic pain, suggesting the model itself shares similar pathophysiology of neuropathic pain. This is further supported by correlation between behavioral changes and the mean theta power in PSD analysis of EEG of which is also reported to be increased in neuropathic pain patients and animal models. Finally, developing the sleep state EEG analysis and additional behavioral analyses measuring mechanical/thermal hypersensitivity/allodynia would be useful to further elucidate the validity of the monkey SNL model as a model of neuropathic pain in the future study.

Conclusion

We demonstrated that the SNL monkey model showed behavioral, EGG score and molecular changes similar to those seen in rodent pain models and patients with neuropathic pain. The transcriptomic analysis of RNA-seq results from the dorsal part of the spinal cord suggested that neuroinflammation and cholesterol transportation/metabolism were the main pathways altered in this NHP model. In conclusion, this study successfully provides a potentially useful pharmacological model that can contribute to the development of pain relief therapies by specifically inducing a robust behavioral phenotype and changes in gene expression resembling those in patients.

Materials and methods

Experimental animals

Eleven male cynomolgus monkeys (*Macaca fascicularis*, 2.5–3.9 kg, provided from and bred at New Drug Research Center Inc., Japan) aged 3–4 years old were used in this study. The animals were kept under light and dark cycles (12/12 h), allowed unrestricted access to tap water, and given 100 g of food (CMK-2; CLEA Japan, Inc., Japan) once a day. The experimental protocol was approved by the experimental animal ethics committees at the New Drug Research Center and Asahi Kasei Pharma Corporation and performed in accordance with established guidelines for the management and handling of experimental animals. This study was performed in accordance with ARRIVE guidelines.

Electrode implant for electroencepharograhy

The animals were anesthetized using 0.1 mg/body (0.2 mL/body, intramuscular injection) of atropine sulfate solution, 5 mg/kg (0.1 mL/kg, intramuscular injection) of ketamine hydrochloride solution, and 1 mg/kg (0.05 mL/kg, intramuscular injection) of xylazine hydrochloride solution. After tracheal cannulation, anesthesia was maintained with 0.1%–5.0% isoflurane during the surgery. The head was fixed in a stereotaxic apparatus, and the skull was exposed after a skin incision. 16 stainless steel screw electrodes (M1.7 mm × 4 mm) including a ground electrode were placed over intact skull corresponding to international 10–20 system. Screws were anchored to the skull using dental cement.

Spinal nerve ligation surgery

The animals were anesthetized using 0.1 mg/body (0.2 mL/body, intramuscular injection) of atropine sulfate solution, 5 mg/kg (0.1 mL/kg, intramuscular injection) of ketamine hydrochloride solution, and 1 mg/kg (0.05 mL/kg, intramuscular injection) of xylazine hydrochloride solution. After tracheal cannulation, anesthesia was maintained with 0.1%–5.0% isoflurane during the surgery. Using an aseptic technique, an incision was made in the skin of the abdomen, the muscle was retracted, and the L7 spinal nerve on the right side was exposed. The right spinal nerve was tightly ligated at two sites distal to the L7 ganglion with 3–0 silk. After the surgery, 250 mg/body of cefazolin sodium and 0.01 mg of buprenorphine were intramuscularly administered once a day for 3 days.

Experimental design

The animals' spontaneous pain was measured by behavioral analysis before the L7 SNL surgery and 1, 2, and 3 months after it (Fig. 1a). All animals were sacrificed via the perfusion of saline under deep anesthesia with ketamine hydrochloride (5 mg/kg, i.m.), xylazine hydrochloride (1 mg/kg, i.m.), and pentobarbital sodium (50 mg/kg, i.v.) 4 months after the surgery. The spinal cord was dissected at the L7 position, separated into the dorsal halves of the left and right sides, immersed in RNAlater solution overnight, and stored at − 80 °C until RNA-seq analysis.

Behavioral testing (weight-bearing)

To evaluate pain-like behavior in the monkey SNL model, we used weight-bearing, which has been used for evaluating spontaneous pain in animal models of neuropathic pain[70]. The animals were acclimated to the experimental room and procedure of testing once a week for at least 8 weeks. Each animal's neck, waist, and forelimbs were fixed on a monkey chair, after which the left and right hindlimbs were individually put on two electric balances (GX-6100R; A&D Company, Ltd., Japan) to measure weight-bearing on each hindlimb. Then, the percentage weight-bearing on the ipsilateral (right) hindlimb was calculated as the weight value on the ipsilateral side divided by the sum of ipsilateral and contralateral weight values using the following formula:

$$\begin{aligned}&\text{Weight-bearing } [\%,\ \text{R} \ /\ (\text{L}+\text{R})] = \text{ ipsilateral weight-bearing (kg)}\\&\times 100 \ /\ [\text{ipsilateral weight-bearing (kg)} + \text{ contralateral weight-bearing (kg)}]\end{aligned}$$

Measurements were performed at around 9:00 a.m. and 1:00 p.m. at each timepoint, and the mean value was calculated.

Electroencepharograhy recording

To evaluate spontaneous pain-like phenotype, we measured theta power in electroencephalography (EEG), which was reported to be enhanced in patients with neurogenic pain and animal models of neuropathic pain[20,22–25]. Each animal's neck, waist, and forelimbs were fixed on a monkey chair, and then the EEG waveform was recorded at a sampling frequency of 1 kHz from the electrodes using 16 ch OmniPlexSystem (Plexon Inc., Dallas, TX).

Power spectral density

Fast Fourier transform was used to convert EEG waveform from the time domain to the frequency domain by using LabChart (ver8, ADInstruments, Dunedin, New Zealand). Mean power values between 4 and 8 Hz (mean theata power) were calculated using the data obtained from C3 electrode (corresponding to primary somatosensory cortex) contralateral to SNL.

Sleeping/waking cycle measurement

To evaluate the effect of SNL surgery on sleep behavior, we measured the sleeping and waking time and the number of sleeping/waking cycles during a dark period (12 h, 19:00–7:00) by visual inspection using video images acquired with cameras set in front of each animal's cage.

Pregabalin treatment

For pharmacological validation of the model, the effect of pregabalin was evaluated using three animals with retained pain-like behavior at 3 months after the surgery. These animals were first subjected to weight-bearing tests just before (at around 9:00 a.m.) and 4 h after the treatment with vehicle (0.5% Methyl Cellulose 400, 0.1 mL/kg, p.o.). At least 3 days after vehicle treatment, weight-bearing tests were done just before and 4 h after the treatment with pregabalin (30 mg/kg, p.o.).

RNA sequencing (RNA-seq) analysis

Sequence libraries were prepared using the TruSeq Stranded mRNA Sample Prep Kit (Illumina, San Diego, CA, USA). Sequencing was performed in the paired-end (150 × 2) mode on NovaSeq (Illumina). The raw sequence data were quality-checked with fastp (version 0.22.0), aligned to the *Macaca fascicularis* 6.0 monkey genome with STAR (version 2.7.9a), and quantified for gene-level counts and transcripts per million (TPM) data using RSEM (version 1.3.1). DESeq2 (version 1.38.3, R version 4.2.3) was used in differential expression analysis.

Metascape (v3.5.20230623, http://metascape.org/) was used for the gene set enrichment analysis and functional annotation. A Metascape analysis is carried out with four sources: Gene Ontology (GO) Biological Processes, Reactome Gene Sets, Kyoto Encyclopedia of Genes and Genomes (KEGG) Pathways[71–73], and Comprehensive Resource of Mammalian Protein Complexes (CORUM). All analyses were performed upon converting the input monkey genes into their human orthologs, as suggested in the Metascape manual.

Immunohistochemistry, and AI-driven fluorescence morphometry

The brains were dissected and fixed in 4% paraformaldehyde at 4 °C for 2 days. After paraffin embedding, paraffin tissue blocks were cut into 5-μm-thick slices. Paraffin-embedded sections were de-paraffinized, and epitope retrieval was performed using a rice steamer at 95 °C for 30 min in 10 mM citrate buffer. The tissue sections were incubated in 5% bovine serum albumin (BSA) (Sigma-Aldrich, St. Louis, MO, USA) in Tris-buffered saline with Tween 20 (TBS-T) (Takara Bio) for 30 min at room temperature and then washed. The samples were then incubated at 4 °C for 15 h in anti-GFAP (1:1000; Abcam, ab7260 Cambridge, UK), or anti-LXRα (1:100; Abcam, ab3585). After being washed, the slides were incubated with goat anti-rabbit IgG (H + L) Alexa Fluor 488 (1:1000; Thermo Fisher Scientific), and DAPI (1:1000; Dojindo Laboratories, Kumamoto, Japan) for 1 h, followed by final washing. Finally, the slides were mounted with coverslips using Prolong Gold antifade mounting medium (Thermo Fisher Scientific).

Imaging of the brain sections stained with immuno-fluorescence was conducted using a Nikon confocal laser microscopy system (A1-ECLIPSE Ti2, Nikon, Tokyo, Japan). An objectives were used: Plan Apo VC 20 × (NA = 0.73, Nikon). Two laser lines at 488 nm and 561 nm for excitation and two filter cubes at 480 nm/560 nm and 560 nm/640 nm for detection were used.

Whole tissue sections from 3 specimens from the 2 experimental groups were imaged. Regions of interest (ROI) of the dorsal horn region were set for morphometrical analyses. Fluorescence morphometry of GFAP-, or LXRα-positive cells was carried out using AI deep learning methods by imaging analysis tools: NIS-Elements AR and NIS, ai (Nikon).

Statistical analyses

All data are presented as the mean ± standard error of mean (SEM). The time-course data from the weight-bearing test were analyzed using repeated measures one-way ANOVA to compare the data among the timepoints. The percentages of ipsilateral weight-bearing at 1, 2, and 3 months after the surgery were compared with the value before the surgery using Dunnett's multiple comparisons test after the confirmation of a significant difference by repeated measures one-way ANOVA. A p-value of < 0.05 was considered statistically significant in the behavioral test.

Data availability

RNA-seq data was deposited into Gene Expression Omnibus (GEO) database under accession number GSE263355 (publicly available in April 2028). The data from the current study is available from Hiroshi Yamane (yamane.hf@om.asahi-kasei.co.jp) upon reasonable request.

Received: 21 March 2024; Accepted: 26 March 2025
Published online: 03 April 2025

References

1. Bouhassira, D., Lantéri-Minet, M., Attal, N., Laurent, B. & Touboul, C. Prevalence of chronic pain with neuropathic characteristics in the general population. *Pain* **136**, 380–387 (2008).
2. Girach, A. *et al.* Quality of life in painful peripheral neuropathies: A systematic review. *Pain Res. Manag.* **2019** (2019).
3. Derry, S. *et al.* Pregabalin for neuropathic pain in adults. *Cochrane Database Syst. Rev.* (2019).
4. Finnerup, N. B. et al. Neuropathic pain clinical trials: Factors associated with decreases in estimated drug efficacy. *Pain* **159**, 2339 (2018).
5. David Thomas, C. a. C. W. *Pain and Addiction Therapeutics*. Vol. 2 (Bio Industry Analysis, 2018).
6. Dworkin, R. H. et al. Considerations for improving assay sensitivity in chronic pain clinical trials: IMMPACT recommendations. *Pain* **153**, 1148–1158 (2012).
7. Gilron, I. Methodological issues associated with clinical trials in neuropathic pain. *Expert. Rev. Clin. Pharmacol.* **9**, 1399–1402 (2016).
8. Dworkin, R. H. et al. Interpreting the clinical importance of treatment outcomes in chronic pain clinical trials: IMMPACT recommendations. *J. Pain* **9**, 105–121 (2008).
9. Dworkin, R. H. et al. Evidence-based clinical trial design for chronic pain pharmacotherapy: A blueprint for ACTION. *Pain* **152**, S107–S115 (2011).
10. Percie du Sert, N. & Rice, A. S. Improving the translation of analgesic drugs to the clinic: Animal models of neuropathic pain. *Br. J. Pharmacol.* **171**, 2951–2963 (2014).
11. Attal, N. & Bouhassira, D. Translational neuropathic pain research. *Pain* **160**, S23–S28 (2019).
12. Bouhassira, D. & Attal, N. Translational neuropathic pain research: a clinical perspective. *Neuroscience* **338**, 27–35 (2016).
13. Palecek, J. et al. Responses of spinothalamic tract neurons to mechanical and thermal stimuli in an experimental model of peripheral neuropathy in primates. *J. Neurophysiol.* **68**, 1951–1966 (1992).
14. Kim, S. H. & Chung, J. M. An experimental model for peripheral neuropathy produced by segmental spinal nerve ligation in the rat. *Pain* **50**, 355–363 (1992).
15. Nagasaka, K., Takashima, I., Matsuda, K. & Higo, N. Brain activity changes in a monkey model of central post-stroke pain. *Exp. Neurol.* **323**, 113096 (2020).
16. Ali, Z. et al. Uninjured C-fiber nociceptors develop spontaneous activity and α-adrenergic sensitivity following L6 spinal nerve ligation in monkey. *J. Neurophysiol.* **81**, 455–466 (1999).
17. Carlton, S. M., Rees, H., Gondesen, K. & Willis, W. D. Dextrorphan attenuates responses of spinothalamic tract cells in normal and nerve-injured monkeys. *Neurosci. Lett.* **229**, 169–172 (1997).
18. Vierck Jr, C. J. & Light, A. R. Allodynia and hyperalgesia within dermatomes caudal to a spinal cord injury in primates and rodents (2000).
19. Boord, P. et al. Electroencephalographic slowing and reduced reactivity in neuropathic pain following spinal cord injury. *Spinal Cord* **46**, 118–123. https://doi.org/10.1038/sj.sc.3102077 (2008).
20. Sarnthein, J., Stern, J., Aufenberg, C., Rousson, V. & Jeanmonod, D. Increased EEG power and slowed dominant frequency in patients with neurogenic pain. *Brain* **129**, 55–64. https://doi.org/10.1093/brain/awh631 (2006).
21. Schulman, J. J., Ramirez, R. R., Zonenshayn, M., Ribary, U. & Llinas, R. Thalamocortical dysrhythmia syndrome: MEG imaging of neuropathic pain. *Thalamus Relat. Syst.* **3**, 33–39 (2005).
22. Stern, J., Jeanmonod, D. & Sarnthein, J. Persistent EEG overactivation in the cortical pain matrix of neurogenic pain patients. *Neuroimage* **31**, 721–731. https://doi.org/10.1016/j.neuroimage.2005.12.042 (2006).
23. Koyama, S. et al. An electroencephalography bioassay for preclinical testing of analgesic efficacy. *Sci. Rep.* **8**, 16402. https://doi.org/10.1038/s41598-018-34594-2 (2018).
24. Koyama, S., Xia, J., Leblanc, B. W., Gu, J. W. & Saab, C. Y. Sub-paresthesia spinal cord stimulation reverses thermal hyperalgesia and modulates low frequency EEG in a rat model of neuropathic pain. *Sci. Rep.* **8**, 7181. https://doi.org/10.1038/s41598-018-25420-w (2018).
25. LeBlanc, B. W., Bowary, P. M., Chao, Y. C., Lii, T. R. & Saab, C. Y. Electroencephalographic signatures of pain and analgesia in rats. *Pain* **157**, 2330–2340. https://doi.org/10.1097/j.pain.0000000000000652 (2016).
26. Ferini-Strambi, L. Neuropathic pain and sleep: A review. *Pain Ther.* **6**, 19–23. https://doi.org/10.1007/s40122-017-0089-y (2017).
27. Cortright, D. N., Matson, D. J. & Broom, D. C. New frontiers in assessing pain and analgesia in laboratory animals. *Expert Opin. Drug Discov.* **3**, 1099–1108. https://doi.org/10.1517/17460441.3.9.1099 (2008).
28. Plante, D. T. Hypersomnia in mood disorders: A rapidly changing landscape. *Curr. Sleep Med. Rep.* **1**, 122–130. https://doi.org/10.1007/s40675-015-0017-9 (2015).
29. Pohóczky, K. et al. Discovery of novel targets in a complex regional pain syndrome mouse model by transcriptomics: TNF and JAK-STAT pathways. *Pharmacol. Res.* **182**, 106347 (2022).
30. Woo, J. et al. PDL241, a novel humanized monoclonal antibody, reveals CD319 as a therapeutic target for rheumatoid arthritis. *Arthritis Res. Ther.* **15**, 1–15 (2013).
31. Sandhir, R., Gregory, E., He, Y.-Y. & Berman, N. E. Upregulation of inflammatory mediators in a model of chronic pain after spinal cord injury. *Neurochem. Res.* **36**, 856–862 (2011).
32. Buckley, D. A. et al. The development of translational biomarkers as a tool for improving the understanding, diagnosis and treatment of chronic neuropathic pain. *Mol. Neurobiol.* **55**, 2420–2430 (2018).
33. Gjefsen, E. et al. Longitudinal changes of serum cytokines in patients with chronic low back pain and Modic changes. *Osteoarthr. Cartil.* **31**, 543–547 (2023).
34. Bäckryd, E. et al. High levels of cerebrospinal fluid chemokines point to the presence of neuroinflammation in peripheral neuropathic pain: A cross-sectional study of 2 cohorts of patients compared with healthy controls. *Pain* **158**, 2487 (2017).
35. Jönsson, M., Gerdle, B., Ghafouri, B. & Bäckryd, E. The inflammatory profile of cerebrospinal fluid, plasma, and saliva from patients with severe neuropathic pain and healthy controls-a pilot study. *BMC Neurosci.* **22**, 1–12 (2021).
36. Thacker, M. A. et al. CCL2 is a key mediator of microglia activation in neuropathic pain states. *Eur. J. Pain* **13**, 263–272 (2009).
37. Piotrowska, A. et al. Direct and indirect pharmacological modulation of CCL2/CCR2 pathway results in attenuation of neuropathic pain—In vivo and in vitro evidence. *J. Neuroimmunol.* **297**, 9–19. https://doi.org/10.1016/j.jneuroim.2016.04.017 (2016).
38. Takada, T. et al. Midkine, a retinoic acid-inducible heparin-binding cytokine in inflammatory responses: Chemotactic activity to neutrophils and association with inflammatory synovitis. *J. Biochem.* **122**, 453–458 (1997).

39. Sakakima, H. et al. Traumatic injury-induced midkine expression in the adult rat spinal cord during the early stage. *J. Neurotrauma* **21**, 471–477 (2004).
40. Ezquerra, L. et al. Different pattern of pleiotrophin and midkine expression in neuropathic pain: Correlation between changes in pleiotrophin gene expression and rat strain differences in neuropathic pain. *Growth Factors* **26**, 44–48 (2008).
41. Wang, Z. et al. Key genes of deficiency of liver and kidney type chronic pain through bioinformatics analyses. *TMR Mod. Herb. Med.* **5**, 7–12. https://doi.org/10.53388/MHM2022A0213001 (2022).
42. Yosten, G. L. et al. GPR160 de-orphanization reveals critical roles in neuropathic pain in rodents. *J. Clin. Investig.* **130**, 2587–2592 (2020).
43. Khan, N. & Smith, M. T. Neurotrophins and neuropathic pain: Role in pathobiology. *Molecules* **20**, 10657–10688. https://doi.org/10.3390/molecules200610657 (2015).
44. Goncalves Dos Santos, G., Delay, L., Yaksh, T. L. & Corr, M. Neuraxial cytokines in pain states. *Front. Immunol.* **10**, 3061. https://doi.org/10.3389/fimmu.2019.03061 (2019).
45. Yousefpour, N. *et al.* Complement protein C1q is a therapeutic target for neuropathic pain (2021).
46. Ray, P. R. et al. RNA profiling of human dorsal root ganglia reveals sex differences in mechanisms promoting neuropathic pain. *Brain* **146**, 749–766 (2023).
47. Gerdle, B. & Ghafouri, B. Proteomic studies of common chronic pain conditions-a systematic review and associated network analyses. *Expert Rev. Proteom.* **17**, 483–505 (2020).
48. Du, H. et al. Analyses of gene expression profiles in the rat dorsal horn of the spinal cord using RNA sequencing in chronic constriction injury rats. *J. Neuroinflamm.* **15**, 1–11 (2018).
49. Barry, A. M., Sondermann, J. R., Sondermann, J.-H., Gomez-Varela, D. & Schmidt, M. Region-resolved quantitative proteome profiling reveals molecular dynamics associated with chronic pain in the PNS and spinal cord. *Front. Mol. Neurosci.* **11**, 259 (2018).
50. Bäckryd, E., Ghafouri, B., Carlsson, A. K., Olausson, P. & Gerdle, B. Multivariate proteomic analysis of the cerebrospinal fluid of patients with peripheral neuropathic pain and healthy controls–a hypothesis-generating pilot study. *J. Pain Res.* 321–333 (2015).
51. Ritter, S. Y. et al. Proteomic analysis of synovial fluid from the osteoarthritic knee: Comparison with transcriptome analyses of joint tissues. *Arthritis Rheum.* **65**, 981–992 (2013).
52. Warwick, C. A., Keyes, A. L., Woodruff, T. M. & Usachev, Y. M. The complement cascade in the regulation of neuroinflammation, nociceptive sensitization, and pain. *J. Biol. Chem.* **297**, 101085. https://doi.org/10.1016/j.jbc.2021.101085 (2021).
53. Farber, K. et al. C1q, the recognition subcomponent of the classical pathway of complement, drives microglial activation. *J. Neurosci. Res.* **87**, 644–652. https://doi.org/10.1002/jnr.21875 (2009).
54. Yang, J. A., He, J. M., Lu, J. M. & Jie, L. J. Jun, Gal, Cd74, and C1qb as potential indicator for neuropathic pain. *J. Cell. Biochem.* **119**, 4792–4798 (2018).
55. Wang, F. et al. Spinal macrophage migration inhibitory factor is a major contributor to rodent neuropathic pain-like hypersensitivity. *J. Am. Soc. Anesthesiol.* **114**, 643–659 (2011).
56. Dorsey, S. G. et al. Whole blood transcriptomic profiles can differentiate vulnerability to chronic low back pain. *PLoS ONE* **14**, e0216539 (2019).
57. Yang, Y. K., Lu, X. B., Wang, Y. H., Yang, M. M. & Jiang, D. M. Identification crucial genes in peripheral neuropathic pain induced by spared nerve injury. *Eur. Rev. Med. Pharmacol. Sci.* **18**, 2152–2159 (2014).
58. Hartlehnert, M. et al. Schwann cells promote post-traumatic nerve inflammation and neuropathic pain through MHC class II. *Sci. Rep.* **7**, 12518. https://doi.org/10.1038/s41598-017-12744-2 (2017).
59. Calvo, M., Dawes, J. M. & Bennett, D. L. The role of the immune system in the generation of neuropathic pain. *Lancet Neurol.* **11**, 629–642. https://doi.org/10.1016/S1474-4422(12)70134-5 (2012).
60. Malcangio, M. Role of the immune system in neuropathic pain. *Scand. J. Pain* **20**, 33–37 (2019).
61. Navia-Pelaez, J. M. et al. Normalization of cholesterol metabolism in spinal microglia alleviates neuropathic pain. *J. Exp. Med.* **218**, e20202059 (2021).
62. Lind, A.-L. *et al.* CSF levels of apolipoprotein C1 and autotaxin found to associate with neuropathic pain and fibromyalgia. *J. Pain Res.* 2875–2889 (2019).
63. Jimenez, C. R. et al. Proteomics of the injured rat sciatic nerve reveals protein expression dynamics during regeneration. *Mol. Cell. Proteom.* **4**, 120–132 (2005).
64. Kim, D.-S. et al. Differentially expressed genes in rat dorsal root ganglia following peripheral nerve injury. *NeuroReport* **12**, 3401–3405 (2001).
65. Lim, T. K. et al. Evidence for a role of nerve injury in painful intervertebral disc degeneration: A cross-sectional proteomic analysis of human cerebrospinal fluid. *J. Pain* **18**, 1253–1269 (2017).
66. Hussain, G. et al. Role of cholesterol and sphingolipids in brain development and neurological diseases. *Lipids Health Dis.* **18**, 1–12 (2019).
67. Krivoi, I. I. & Petrov, A. M. Cholesterol and the safety factor for neuromuscular transmission. *Int. J. Mol. Sci.* **20**, 1046 (2019).
68. Iqbal, Z. et al. Lipids and peripheral neuropathy. *Curr. Opin. Lipidol.* **32**, 249–257 (2021).
69. Dai, L. et al. Cholesterol metabolism in neurodegenerative diseases: Molecular mechanisms and therapeutic targets. *Mol. Neurobiol.* **58**, 2183–2201 (2021).
70. Tappe-Theodor, A. & Kuner, R. Studying ongoing and spontaneous pain in rodents–challenges and opportunities. *Eur. J. Neurosci.* **39**, 1881–1890. https://doi.org/10.1111/ejn.12643 (2014).
71. Kanehisa, M. & Goto, S. KEGG: Kyoto encyclopedia of genes and genomes. *Nucleic Acids Res.* **28**, 27–30. https://doi.org/10.1093/nar/28.1.27 (2000).
72. Kanehisa, M. Toward understanding the origin and evolution of cellular organisms. *Protein Sci.* **28**, 1947–1951. https://doi.org/10.1002/pro.3715 (2019).
73. Kanehisa, M., Furumichi, M., Sato, Y., Kawashima, M. & Ishiguro-Watanabe, M. KEGG for taxonomy-based analysis of pathways and genomes. *Nucleic Acids Res.* **51**, D587-d592. https://doi.org/10.1093/nar/gkac963 (2023).

Acknowledgements

The authors thank Shunichi Kitajima, Chihomi Mitsuoka, Sachi Okabayashi, and Takashi Sakuraba of New Drug Research Center, Inc., for their support to conduct in vivo experiments. The authors also express sincere thanks to Atsushi Toyoda of National Institute of Genetics for their expertise in RNA-seq analysis. The authors are also grateful to members at Department of Pharmacology, Faculty and Graduate School of Dental Medicine, Hokkaido University for their helpful comments on this work, and Edanz (https://jp.edanz.com/ac) for editing a draft of this manuscript. This study was funded by the Asahi Kasei Pharma Corporation. This work was also supported by a Grant-in-Aid for Scientific Research from the Japan Society for the Promotion of Science (JSPS KAKENHI), Grant Number 23K18347, and 24KK0165 to Tadahiro Iimura, and by JSPS KAKENHI Grant-in-Aid for Early-Career Scientists to H. Watanabe. This work was also supported by JST SPRING, Grant Number JPMJSP2119 to R. Koguchi, H. Watanabe, and M. Nishiura.

Author contributions

Hiroshi Yamane: Conceptualization, Methodology, Validation, Formal analysis, Investigation, Writing—Original draft. Suguru Koyama: Conceptualization, Methodology. Takayuki Komatsu: Methodology. Tomoya Tanaka: Formal analysis. Riyu Koguchi: Methodology, Validation, Formal analysis, Investigation. Haruhisa Watanabe: Methodology, Validation, Formal analysis, Investigation, Writing-review editing. Mai Nishiura: Writing-review editing. Satoru Yoshikawa: Supervision, Project administration, Writing—Reviewing and editing. Tadahiro Iimura: Supervision, Writing—Reviewing and editing.

Declarations

Competing interests

Hiroshi Yamane, Suguru Koyama, Takayuki Komatsu, Tomoya Tanaka, and Satoru Yoshikawa are employees of Asahi Kasei Pharma Corporation. Riyu Koguchi, Haruhisa Watanabe, Nishiura Mai, and Tadahiro Iimura declare no conflicts of interest.

Additional information

Supplementary Information The online version contains supplementary material available at https://doi.org/10.1038/s41598-025-96160-x.

Correspondence and requests for materials should be addressed to H.Y., S.Y. or T.I.

Reprints and permissions information is available at www.nature.com/reprints.

Publisher's note Springer Nature remains neutral with regard to jurisdictional claims in published maps and institutional affiliations.